

****Volume Title****
*ASP Conference Series, Vol. **Volume Number***
****Author****
 © ****Copyright Year**** *Astronomical Society of the Pacific*

A small slice of the Milky Way disk in SDSS

Martin C. Smith^{1,2}

¹*Kavli Institute for Astronomy and Astrophysics, Peking University, Beijing 100871, China; msmith@pku.edu.cn*

²*National Astronomical Observatories, Chinese Academy of Sciences, Beijing 100012, China*

Abstract. The present-day state of the Milky Way disk can tell us much about the history of our Galaxy and provide insights into its formation. We have constructed a high-precision catalogue of disk stars using data from the Sloan Digital Sky Survey (SDSS) and use these stars to probe the heating history as well as investigating the detailed phase-space distribution. We also show how this sample can be used to probe the global properties of the Milky Way disk, employing the Jeans equations to provide a simple model of the potential close to the disk. Our model is in excellent agreement with others in the literature and provides an indication that the disk, rather than the halo, dominates the circular speed at the solar neighborhood. The work presented in these proceedings has been published as “Slicing and dicing the Milky Way disc in SDSS” (Smith et al. 2012).

1. Introduction and sample construction

Large surveys such as SDSS are beginning to enable detailed studies to be made of the properties of the Milky Way. It is now possible to construct high-precision catalogues of stars with full 3D kinematics and from these analyse the structure and evolution of our Galaxy. In the following proceedings I summarise our study of the disk of the Milky Way (presented in full in Smith et al. 2012), highlighting two of the most important results.

We use data from the 7th public data release of the SDSS, concentrating on the 250 square degree Stripe 82 region for which it is possible to obtain high precision photometry and proper motions (Bramich et al. 2008). This catalogue has been exploited in a variety of works, covering white dwarfs (Vidrih et al. 2007), halo kinematics (Smith et al. 2009a,b) and RR Lyrae in the outer halo (Watkins et al. 2009).

We take all dwarf stars with good quality spectra (Lee et al. 2008), estimating distances using a slightly modified version of the Ivezić et al. (2008) photometric parallax relation. Our modification concerns the turn-off correction (equation A6 of Ivezić et al. 2008), which we argue is not applicable to disk stars (see the Appendix of Smith et al. 2012). We then calculate the three-dimensional velocities for our sample, propagating all uncertainties, and obtain final errors of around 20 to 30 km s⁻¹ for each component of the velocity.

As we are interested in the kinematics of the disk as a function of height from the plane, we restrict ourselves to $7 \leq R \leq 9$. We also split the data into three ranges in

metallicity ($-1.5 \leq [\text{Fe}/\text{H}] \leq -0.8$, $-0.8 \leq [\text{Fe}/\text{H}] \leq -0.5$ and $-0.5 \leq [\text{Fe}/\text{H}]$), and then for each metallicity bin we further divide the data into four ranges in z out to a maximum distance of 2 kpc. The stars are equally divided between the four distance bins, resulting in around 500 to 800 stars per bin from our full sample of 7280 stars. This binning is necessary in order to avoid having to model the SDSS spectroscopic selection function.

Once we have divided up our stars, we then proceed to fit the distribution of kinematics using maximum likelihood methods (incorporating the uncertainties on the individual velocities). Both v_R and v_z are fit using Gaussian distributions, but since it is well known that the distribution of v_ϕ for the disk is highly skewed and non-Gaussian we adopt an asymmetric functional form (equation (15) of Cuddeford & Binney 1994). When carrying out this analysis it is crucial to remove contamination from halo stars, particularly for the most metal-poor bins. We do this by including a non-rotating Gaussian component into the velocity fits, where the level of contamination (and hence amplitude of the Gaussian) is assumed to be twice the number of counter-rotating stars. The halo dispersions are fixed according to the values found in Smith et al. (2009a).

2. The rotation lag of the disk and the asymmetric drift

A comprehensive analysis of the results are presented in Smith et al. (2012). Here we concentrate on the most important properties, starting with rotation lag. We are able to trace the lag (Fig. 1) to a couple of kpc outside the plane and find that it follows the well-known asymmetric drift relation. The hotter (metal-poor) stars exhibit greater lag than the colder (metal-rich) populations, resulting in a clear correlation between lag and metallicity. The gradient of the lag with respect to $|z|$ varies from around 15 to 40 $\text{km s}^{-1} \text{kpc}^{-1}$, depending on metallicity. Fig. 1 also shows how the lag is correlated with σ_R^2 . For the solar-neighbourhood it is known that this is a linear relation (Dehnen & Binney 1998a), but as we can see from our figure this is no longer true once we move beyond 0.5 kpc. However, it can be seen that there is still a relatively tight correlation with σ_R^2 , which is independent of metallicity.

3. Constraining the gravitational potential of the disk

As has been shown by many authors, most notably in the seminal work of Kuijken & Gilmore (1991), the vertical velocity dispersion profile can be used to constrain the gravitational potential of the disk. We show the results derived from our data in Fig. 2, where we have included an additional solar-neighbourhood metal-rich data point derived from the Geneva-Copenhagen survey (Nordström et al. 2004). We take a simplified two-parameter model for the potential, consisting of an infinite razor-thin sheet embedded in a constant background. Our best-fit model estimates that the mass density of these two components are $32.5 \text{ M}_\odot \text{pc}^{-2}$ and $0.015 \text{ M}_\odot \text{pc}^{-3}$, respectively.

As can be seen from Fig. 2, our measurement of the potential is in good agreement with existing models, especially Model 1 of Dehnen & Binney (1998b). This is the least halo-dominated model of Dehnen & Binney (1998b), with the disk (which has a relatively short scale-length) dominating the circular speed at the solar neighborhood. Interested readers should consult section 2.7 of Binney & Tremaine (2008) for a detailed comparison of these models.

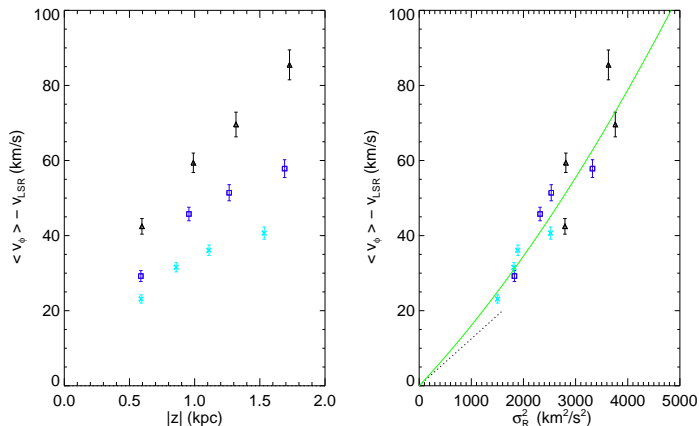


Figure 1. The rotational lag, plotted against z (left) and against the radial velocity dispersion (right). The triangles, squares and crosses correspond to metal-poor, intermediate-metallicity and metal-rich populations, respectively. The dotted line in the right panel corresponds to the solar-neighborhood relation from Dehnen & Binney (1998a) and the solid line denotes an empirical fit with the lag equal to $0.0149\sigma_R^2 + 1.21 \times 10^{-6}\sigma_R^4$. Figure taken from Smith et al. (2012).

Note that this background mass density is close to the $0.014 M_\odot \text{pc}^{-3}$ predicted using isothermal spherical halo models (equation 4.279 of Binney & Tremaine 2008). If we assume our background mass represents the dark halo, it corresponds to a local dark matter density of 0.57 GeV cm^{-3} , which is noticeably larger than the canonical value of 0.30 GeV cm^{-3} typically assumed (e.g. Jungman et al 1996). Our analysis adds still more weight to the argument the local halo density may be substantially underestimated by this generally accepted value. Perhaps more robust than the local mass density is the surface mass density. By integrating our mass distribution we obtain a total surface mass density of $\Sigma_{1.1\text{kpc}} = 66 M_\odot \text{pc}^{-2}$, which agrees well with the classical value of $71 \pm 6 M_\odot \text{pc}^{-2}$ from Kuijken & Gilmore (1991). If we integrate beyond 1.1 kpc, we find $\Sigma_{2\text{kpc}} = 94 M_\odot \text{pc}^{-2}$ and $\Sigma_{4\text{kpc}} = 155 M_\odot \text{pc}^{-2}$.

4. Conclusion

Our results (presented in full in Smith et al. 2012) can be used to address the global properties of the disk and also the heating processes that have shaped its evolution. In order to fully understand the nature of disk heating and to disentangle the contributions from various mechanisms, one needs to go beyond the work presented here. The most crucial improvement will be the ability to make direct estimates for stellar ages, rather than relying on correlations with metallicity. One aspect that will help us in this effort is by folding in measurements of alpha-element abundances that are now being determined routinely for vast numbers of stars (e.g. Lee et al. 2011).

Question: (Nicolas Martin) Can you develop your model to test for the presence of a dark disk (e.g. Read et al. 2008)? **Reply:** Due to the limitations of the data that we have used there are a number of uncertainties in our modelling. As a consequence of these limitations, I think it would be difficult to include extra parameters.

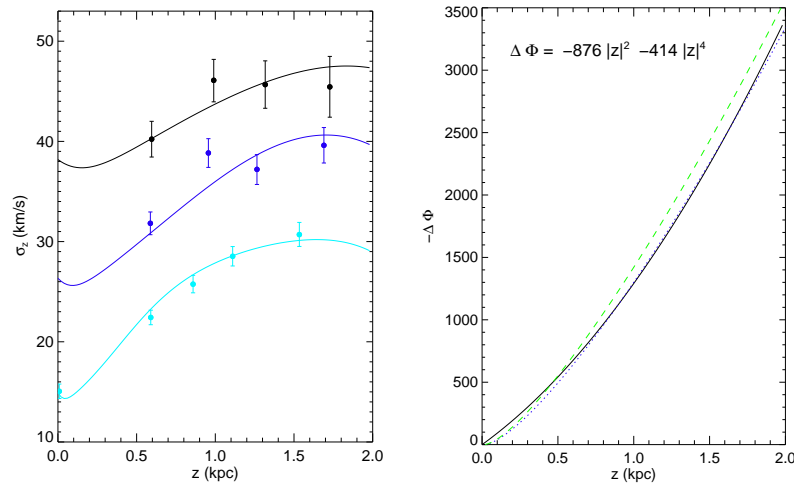


Figure 2. The results of our modeling of the potential of the Galactic disk. The left panel shows the vertical velocity dispersion profiles (metal-poor - top; metal-rich - bottom), along with the corresponding profiles for the potential (solid lines). The right panel shows the potential resulting from this model. For the purposes of comparison we have included models for the potential taken from Dehnen & Binney (1998 – Model 1, dotted; Model 4, dashed). Figure adapted from Smith et al. (2012).

Acknowledgments. MCS acknowledges financial support from the Peking University One Hundred Talent Fund (985) and NSFC grants 11043005 and 11010022. This work was also supported by the European Science Foundation (ESF) for the activity entitled ‘Gaia Research for European Astronomy Training’.

References

- Binney, J.J., & Tremaine, S. 2008, *Galactic Dynamics*. Princeton Univ. Press, Princeton, NJ
- Bramich, D.M., Vidrih, S., Wyrzykowski, L., et al. 2008, *MNRAS*, 386, 887
- Cuddeford, P., & Binney, J. 1994, *MNRAS*, 266, 273
- Dehnen, W., & Binney, J.J. 1998a, *MNRAS*, 298, 387
- Dehnen, W., & Binney, J.J. 1998b, *MNRAS*, 294, 429
- Ivezić, Z., Sesar, B., Jurić, M., et al. 2008, *ApJ*, 684, 287
- Jungman, G., Kamionkowski, M., Griest, K., 1996, *Phys. Rep.*, 267, 195
- Kuijken, K., & Gilmore, G. 1991, *ApJ*, 367, L9
- Lee, Y.S., Beers, T.C., Sivarani, T., et al. 2008, *AJ*, 136, 2022
- Lee, Y.S., Beers, T.C., A., D., et al. 2011, *ApJ*, 738, 187
- Nordström, B., Mayor, M., Andersen, J., et al. 2004, *A&A*, 418, 989
- Read, J.I., Lake, G., Agertz1, O., Debattista, V.P. 2008, *MNRAS*, 389, 1041
- Smith, M.C., Evans, N.W., Belokurov, V., et al. 2009a, *MNRAS*, 399, 1223
- Smith, M.C., Evans, N.W., An, J.H. 2009b, *ApJ*, 698, 1110
- Smith, M.C., Whiteoak, S.H., Evans, N.W. 2012, *ApJ*, in press (arXiv:1111.6920)
- Vidrih, S., et al. 2007, *MNRAS*, 382, 515
- Watkins, L.L., et al. 2009, *MNRAS*, 398, 1757